Nucl. Phys. A 1058 (2025) 123040

Contents lists available at ScienceDirect

Nuclear Physics A

journal homepage: www.elsevier.com/locate/nuclphysa

Quasifission and deep inelastic collisions competing with superheavy element creation

D.J. Hinde [a,*], D.Y. Jeung [a], M. Dasgupta [a], J. Buete [a], K.J. Cook [a], C. Simenel [a,b], E.C. Simpson [a], H.M. Albers [c], Ch.E. Düllmann [c,d,e], J. Khuyagbaatar [c,d], A. Yakushev [c,d]

[a] Department of Nuclear Physics and Accelerator Applications, Research School of Physics, Australian National University, Canberra, ACT 2601, Australia
[b] Department of Fundamental and Theoretical Physics, Research School of Physics, Australian National University, Canberra, ACT 2601, Australia
[c] SHE Chemistry Department, GSI Helmholtzzentrum fur Schwerionenforschung, Darmstadt, 64291, Germany
[d] SHE Chemistry Section, Helmholtz Institute Mainz, Mainz, 55099, Germany
[e] Department of Chemistry - TRIGA Site, Johannes Gutenberg-Universitat Mainz, Mainz, 55099, Germany

ARTICLE INFO

Keywords:
Superheavy elements
Quasifission mass distributions
Sequential fission
Shell effects

ABSTRACT

Fusion forming superheavy elements is strongly inhibited by the faster non-equilibrium Deep Inelastic (DIC) and quasifission processes. These have often been considered as distinct processes, but recent measurements for reactions involving heavy nuclei such as ^{208}Pb and lighter suggest that these two processes form a continuum. However, for reactions of heavy ions with actinide nuclei, binary mass-split spectra show reduced yields for fragments lighter than the target, resulting in a peak in yield close to ^{208}Pb. This gives an apparent separation between DIC and quasifission outcomes. The ^{208}Pb peak has generally been attributed to the ^{208}Pb closed shells giving a valley in the potential energy surface, attracting quasifission trajectories. However, recent extensive binary and three-body cross-sections extracted for reactions of ^{50}Ti with actinide nuclides could not be explained in this framework. Rather, the big drop in yield observed for the heavier actinide targets is consistent with sequential fission of heavy deep inelastic/quasifission fragments.
To search for shell effects in quasifission independent of sequential fission, systematics of mass spectra in non-actinide reactions forming actinide compound nuclei were studied. These showed negligible effects of the shells *known* to cause low energy mass-asymmetric fission of these nuclei. All these results raise questions over the understanding of the effects of closed shells on the quasifission mechanism, and quasifission mass distributions.

1. Introduction

Super-Heavy Elements (SHE) are synthesised by nuclear fusion reactions. To achieve fusion, the two nuclei must first be brought into contact, so that nuclear interactions are initiated. Subsequently, following dissipation of kinetic energy, the nuclear surfaces "stick" together, and the shape of the combined system must then evolve from the *elongated* configuration at contact to the *compact* superheavy compound nucleus (CN), that is only stabilised by local shell effects. This probability P_{CN} is small [1–6] because the

* Corresponding author.
E-mail address: david.hinde@anu.edu.au (D.J. Hinde).

https://doi.org/10.1016/j.nuclphysa.2025.123040
Received 13 October 2024; Accepted 12 February 2025

Available online 17 February 2025

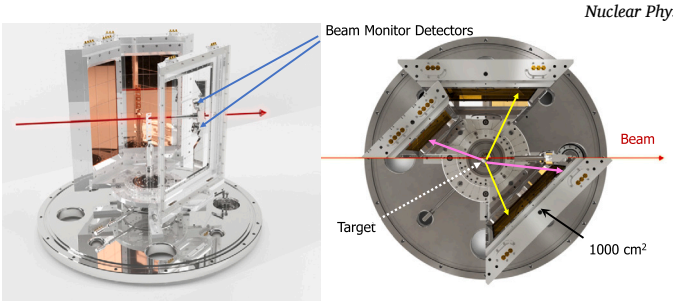

Fig. 1. 3-D perspective rendering (left) and plan view (right) of the CUBE detector setup used for the measurements. The active area of a detector is 1000 cm^2. Examples of pairs of (two-body) fission fragment trajectories are shown by yellow and pink pairs of arrows. (Produced by T. Tunningley, ANU.) (For interpretation of the colours in the figure(s), the reader is referred to the web version of this article.)

total potential after contact is generally repulsive [7]. This favours two faster (10^{-21} to 10^{-20} s) [8–17] non-equilibrium processes. Deep inelastic scattering is fastest, during which energy damping occurs [18], but masses remain close to those of the projectile and target. Quasifission [19,20,8,5,21] has longer sticking times, and shows essentially fully-damped kinetic energies, with masses evolving towards the energetically-favoured symmetric mass-splits. Much effort has been directed [21] to understanding the factors that affect the trajectories over the potential energy surface, since these in turn determine P_{CN}.

A key characteristic of quasifission seen in many reactions with actinide nuclides (used to synthesise all the heaviest elements) is a peak in the binary quasifission yield [1,12,22–27] near ^{208}Pb – a nucleus having enhanced binding since its 82 protons and 126 neutrons fill spherical quantum shells. These experimental observations, in conjunction with model calculations, led to the view that the ^{208}Pb valley in the potential energy surface is responsible for the peak, attracting or intercepting [7,12,22,28,26] trajectories over the PES that might otherwise result in formation of a compact superheavy nucleus. Two outcomes of this picture should result: *enhancement* of the quasifission yield near ^{208}Pb, and reduction of P_{CN}.

This interpretation of the origin of the ^{208}Pb peak conflicts with an early work [29] suggesting that sequential fission could be an important factor. Sequential fission, a well-established process [30,31,29,32–34], occurs when a fissile heavy nucleus produced in an initial (primary) reaction (e.g. a transfer reaction) subsequently decays by fission. This results in a three-body rather than binary outcome. However, slightly later experimental results [20], also for reactions with ^{238}U, claimed sequential fission has a negligible effect. Subsequently, sequential fission had not been considered as an explanation of the ^{208}Pb peak [7,12,22,28,26]. However, the effect of sequential fission on total capture cross-sections was recently discussed [35,36].

As described in Ref. [37], an experimental study was recently carried out to address these conflicting assumptions and interpretations of the effect of shells in quasifission, for reactions of ^{50}Ti with actinide nuclides from ^{232}Th to ^{249}Cf. The aim was to determine – from absolute cross-sections – whether the low yields of binary quasifission fragments heavier than ^{208}Pb result mainly (a) from trajectories being *attracted* to the ^{208}Pb valley, or (b) from the sequential fission of heavier fragments that are produced in the *primary* reaction process. The latter would result in a three-body outcome, leading to *suppression* of products heavier than ^{208}Pb in measured *binary* quasifission mass spectra. These scenarios should be distinguishable, because sequential fission would result in *reduced* total binary quasifission cross sections.

2. Experiment

Experiments were carried out at the ANU Heavy Ion Accelerator Facility, using pulsed beams [38,39] of ^{50}Ti bombarding targets of ^{232}Th, ^{238}U, ^{244}Pu, ^{248}Cm and ^{249}Cf at beam energies from 0.98 to 1.15 of calculated [40] capture barrier energies V_B. Targets comprised 30-160 μg/cm^2 of the actinide material, deposited on 115-280 μg/cm^2 Al or Al/Ti [15] backing foils. Pairs of fission fragments, identified both by their individual and correlated velocities, were detected in coincidence using the CUBE detector system [41,42,11,15] (see Fig. 1). The large position-sensitive MWPCs gave scattering angle coverage of $10° \lesssim \theta \lesssim 80°$ on one side of the beam axis, and $55° \lesssim \theta \lesssim 169°$ on the other. Beam monitor detectors were located at ± 22.5° for cross-section normalization.

Fission fragments pairs can arise (a) from two-body final states (quasifission and fusion-fission), or (b) from three-body final states consisting of a projectile-like nucleus and two fission fragments following sequential fission of a target-like nucleus [36]. These are sketched in Fig. 2(a), and can be separated using the co-linearity of the two-body fragments in the centre-of-mass frame of the collision [36,41,11,43]. In practice, binary events were selected within the blue-white dashed elliptical gate at the centre of Fig. 2(b).

3. Experimental results

A binary quasifission mass-angle distribution (MAD) is shown in Fig. 2(c). The MAD represents the two-body double differential cross-section $d^2\sigma_{2B}/dM_R d\theta_{c.m.}$ as a function of M_R and $\theta_{c.m.}$.

The MAD shows scattering events centred on the projectile-target mass-ratio, indicated by the long dashed lines. Binary quasifission yields are peaked close to ^{208}Pb (dotted lines), with the projectile-like mass distribution extending to or beyond [16] mass-symmetry. Quasifission events are peaked in angle, indicating a short sticking time of ∼5 zs, a typical value for all these and similar [44,45,11,46,15] reactions. There is a strong reduction in quasifission yield as M_R values approach the projectile/target masses, most visible

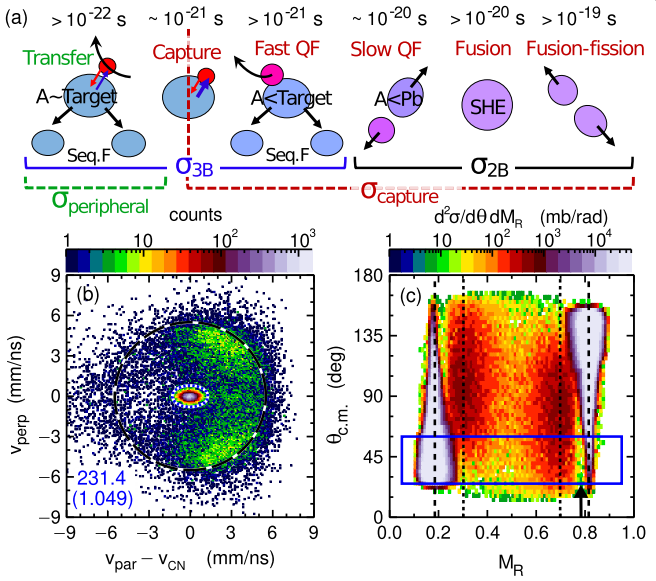

Fig. 2. (a) Two-body (2B) fission and quasifission (QF), and three-body (3B) sequential-fission (Seq. F) mechanisms, characteristic times, with identification of experimental and conceptual (perepheral and capture) cross-sections σ. (b) Fission source velocity distribution [41,11,43,36] for all angles, for the ^{50}Ti+^{248}Cm reaction at $E_{c.m.}$ = 231.4 MeV, 1.049 times the calculated [40] capture barrier energy V_B. The central dashed ellipse selects binary events. The large dashed circle is the boundary for sequential fission when the projectile-like ejectile has the beam momentum. (c) Measured mass ratio vs. angle distribution (MAD) for binary events. Vertical long-dashed lines show the entrance-channel mass-ratio, dotted lines show a ^{208}Pb quasifission fragment. The arrow at M_R = 0.79 indicates the region of missing events, attributed to sequential fission. Mass-spectra in Fig. 5 are for 25° < $\theta_{c.m.}$ < 60° (blue rectangle). Adapted from Ref. [37].

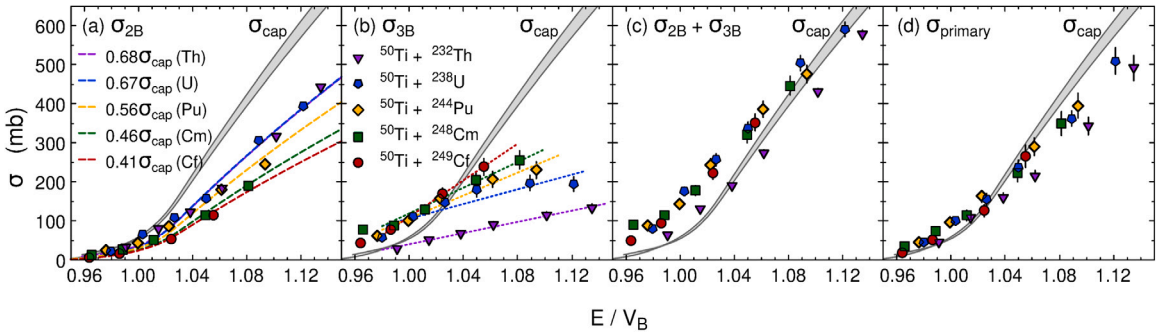

Fig. 3. Cross-sections of two-body (a), estimated three-body (b), and summed two- and three-body fission (c) compared with capture calculations (grey band). The extrapolated primary quasifission cross-sections (see text) is compared in (d).

at angles where the heavy target-like scattering recoils are weakest, as indicated at the bottom of Fig. 2(c) by the black arrow. Mass projections for the angular range 25° < $\theta_{c.m.}$ < 60° (blue rectangle) are presented in Fig. 4, and will be discussed in Sect. 3.3. For $\theta_{c.m.}$ >90°, large scattering yields mask this mass range. Since the angular distributions for other quasifission masses are essentially mass-independent, it seems reasonable that this feature is present for $\theta_{c.m.}$ > 90°.

3.1. Two-body cross sections

Total binary (2-body) quasifission cross-sections σ_{2B} were obtained by integrating the measured quasifission angular distributions [extracted from the MADs such as shown in Fig. 2(c)]. Extrapolation to 0° and 180° was achieved by fitting with an empirical model of quasifission angular distributions [36]. Due to the wide experimental angular coverage, this extrapolation only added a small contribution.

In Fig. 3(a) the σ_{2B} for each reaction are shown as a function of E/V_B, where V_B was calculated from Ref. [40]. The calculated capture cross-sections for reactions with each target are very similar at the same E/V_B (each being within the grey band), but the experimental σ_{2B} are different for each reaction. They fall significantly with increasing target Z, matching calculations only after scaling the calculations (dashed curves) by factors decreasing from 0.68 for ^{232}Th to 0.41 for ^{249}Cf.

This reduction with increasing target Z is inconsistent with trajectories being attracted to the ^{208}Pb valley. That mechanism should change the mass spectra, but *not* σ_{2B}. However, it might be consistent with an increasing fraction with increasing target Z of the primary binary quasifission yield undergoing sequential fission. These events are rejected by the binary event condition in the

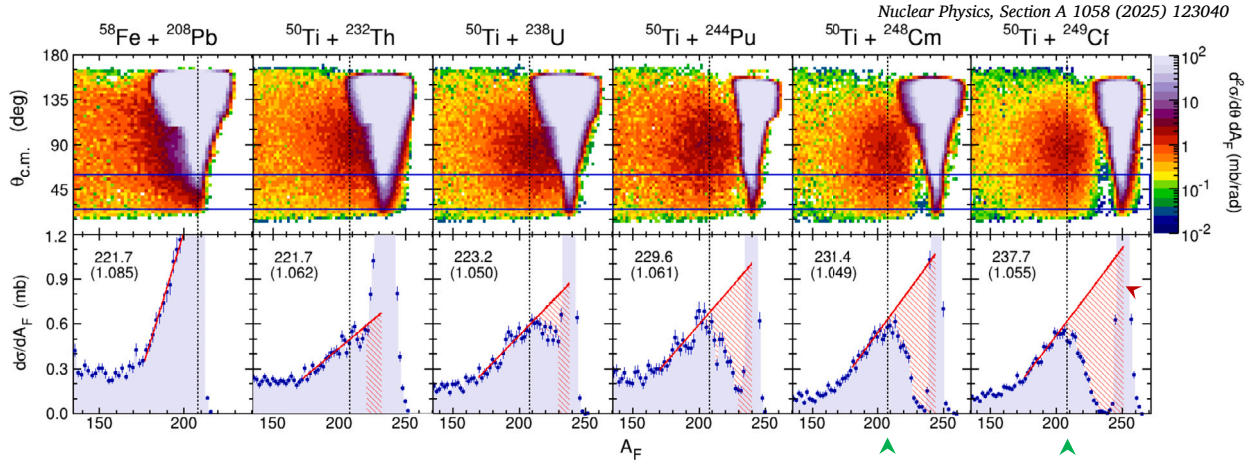

Fig. 4. The upper panels show the heavy-mass part of the two-body MADs for the indicated reactions. The c.m. energies are shown in the lower panels, along with the values of E/V_B (in brackets), which are all close to 1.05. Mass spectra for the angular range $25° < \theta_{c.m.} < 60°$ (boundaries shown by the blue horizontal lines) – where scattering events are not too intense to obscure the quasifission – are shown in the panels below. There is an increasing gap between scattering events and quasifission for fragment masses above ^{208}Pb (dotted lines) as the *target* mass increases. The dotted lines (highlighted by green arrowheads) indicate mass 208.

analysis. This increase is physically reasonable because the fraction of fissile actinide quasifission fragments produced in the primary quasifission process should be larger for higher-Z targets [37].

3.2. Three-body cross sections

This interpretation is supported by the estimation of sequential fission yields from the fission coincidence data. Fig. 2(b) shows that the two-body and three-body fission events are clearly separated using the deduced fission source velocity components. However, to estimate the three-body cross-sections, difficulty arises because the correlation angles of sequential fission fragments can be widely spread as a result of the high momentum of the associated beam-like ejectile [36]. The CUBE detector angular coverage in these measurements is large enough to allow this to be overcome without total reliance on a simulation of coincidence efficiency. By selecting a specific limited range in lab. frame scattering and azimuthal angles of one sequential fission fragment, it was demonstrated [36] that the second fragment was detected with full geometrical efficiency in the other detector for scattering angles corresponding to mean centre-of-mass angles $\theta_{c.m.} \sim 105°$. Around this angle, pairs of fission fragments from *both* binary and three-body events were detected with full efficiency. Following the procedure described in Ref. [37], total three-body cross-sections σ_{3B} were extracted.

These σ_{3B} are shown in Fig. 3(b). At $E/V_B \sim 1$ they are similar for all but ^{50}Ti + ^{232}Th. This similarity is consistent with mainly non-capture origins at such energies, specifically sequential fission following nucleon and multi-nucleon transfer (MNT). The lower values for ^{232}Th may well be a result of the higher fission barriers for MNT products lighter than Th. At higher E/V_B, σ_{3B} increases with increasing target Z such that for the ^{248}Cm and ^{249}Cf reactions, $\sigma_{3B} > \sigma_{2B}$. This observation is consistent with the suggestion that sequential fission is responsible for the observed reduction in σ_{2B} with increasing target Z.

The sum of σ_{2B} and σ_{3B} is compared with σ_{cap} in Fig. 3(c). Each reaction (except for the least-fissile target nuclide ^{232}Th) shows very similar cross sections over the whole energy range, indicating that the reduction in σ_{2B} with increasing target Z is indeed associated with increasing sequential fission. Experimental $\sigma_{2B} + \sigma_{3B}$ values are close to σ_{cap} at higher energies, but larger at near-barrier energies. The latter might be expected, since non-capture events will contribute increasingly to σ_{3B} when E/V_B decreases [47,48].

The measured σ_{2B} and σ_{3B} indicate there is a large cross-section of sequential fission following capture, increasing with target Z. This is consistent with a scenario where heavy (actinide) nuclei produced in *primary* very mass-asymmetric quasifission events subsequently undergo sequential fission, resulting in three-body events. This process is illustrated schematically in Fig. 2(a). The measurements show that this fraction increases with increasing target Z (and thus fissility), as would be expected.

3.3. Estimating primary quasifission cross sections

In contrast to the actinide reactions, our measurement for the ^{58}Fe+ ^{208}Pb reaction (left panel of Fig. 4) shows a continuously rising binary reaction yield up to the target mass. This reaction has a similar charge product, implying similar quasifission dynamics [11]. In this reaction sequential fission is very unlikely at near-barrier energies because of the high fission barriers around ^{208}Pb. Thus this result can be used as a guide to the *primary* quasifission mass distribution for the reactions of ^{50}Ti with the actinide targets. Assuming a linear dependence up to the target mass (red lines fitted to the mass range A = 170 to 200) provides an estimated total primary quasifission cross-section. The "missing" cross-section above the blue experimental data points is attributed to sequential fission, resulting in three-body events, and is shown by red hatching. This includes the region close to the target mass where two-body quasifission events are obscured by the large quasielastic yield. Summing the red-hatched region with the experimental binary quasifission yield (shaded blue) allows an estimate of the primary quasifission cross section $\sigma_{primary}$. These cross-sections are shown

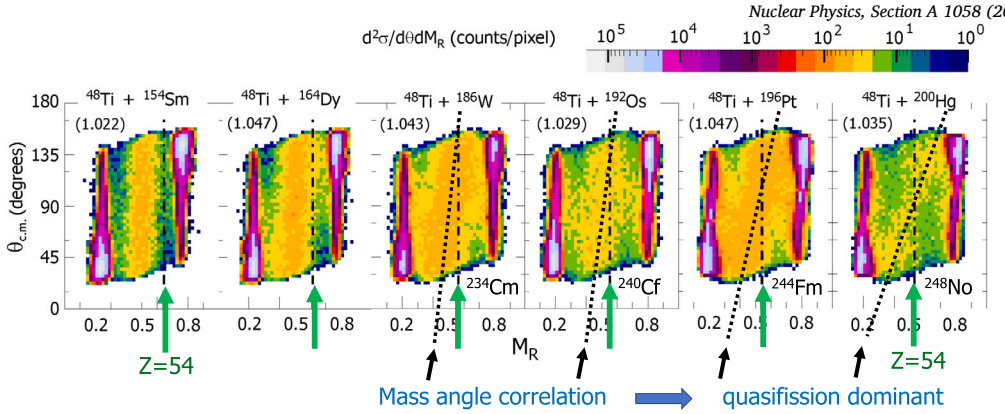

Fig. 5. Mass-angle distributions (MADs) from representative reactions with the lighter targets, and for all targets heavier than ^{178}Hf that were measured. Fission and quasifission lie between the intense quasielastic bands occurring at the mass-ratios $M_R \sim 0.2$ and 0.8. The MADs indicate a transition from dominantly fusion-fission for ^{154}Sm to dominantly quasifission for ^{186} W and heavier targets. The MAD for ^{48}Ti+ ^{164}Dy suggests the presence of both components with similar yields. The values of E/V_B are given in brackets (see text). The mass-ratio M_R values corresponding to a heavy fragment with Z = 54 are indicated by the vertical dot-dashed lines. No clear evidence for enhancements in yield around Z = 54 is seen in the MADs.

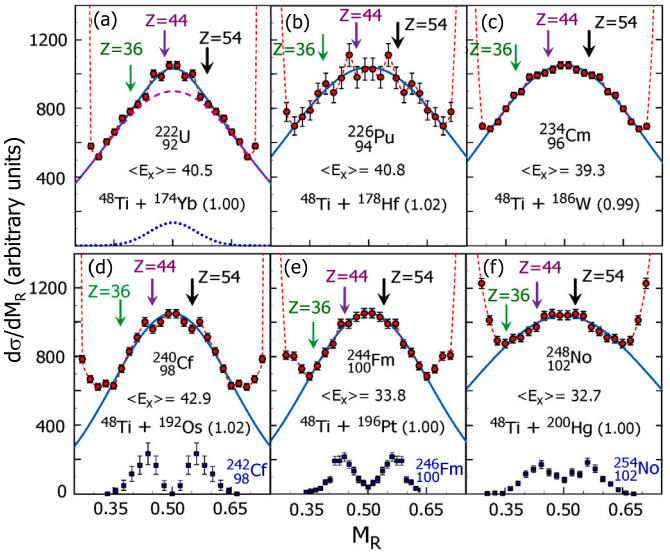

Fig. 6. Adapted from Ref [49]. Mass-ratio M_R spectra averaged over the lowest two or three beam energies for the heavier target measurements. The resulting average excitation energies above the ground-states $<E_x>$ and E/V_B (brackets) are indicated. The compound nucleus is indicated for each reaction. Gaussian fits are indicated by blue curves (total). Narrow (blue dotted) and wide (dashed magenta) Gaussians were required for ^{222}U (panel (a)), where fusion-fission and quasifission both contribute significantly. The vertical arrows show the M_R values corresponding to the indicated proton numbers believed to affect fusion-fission (see text). In (d) to (f), mass spectra for low energy fission [50–52] of neighbouring nuclides (identified in blue text) are also plotted, showing the dominant role of shells around Z = 54 for these nuclei. For the quasifission reactions, one or more data points for M_R values slightly above Z = 54 lie just above the Gaussian fits. If this results from shells, their effect is clearly small at the excitation energies of these measurements.

in Fig. 3(d). There is strong consistency between these cross-sections for each target, and reasonable agreement with the calculated capture cross-sections (grey shaded band).

The consistency for the different reactions demonstrates that the drop in the measured binary quasifission yield between the ^{208}Pb peak and the target mass is the reason for the reduction in σ_{2B} as the target Z increases (Fig. 3(a)). Furthermore, the σ_{3B} results show that these missing experimental cross-sections (corresponding to fissile actinide *primary* quasifission fragments) appear in the experimental three-body sequential fission cross-sections. All results are thus consistent with the importance of sequential fission in these reactions.

4. Shell effects in non-actinide quasifission

In another approach to investigate the role of shell effects in quasifission, Ref. [49] showed the results of measurements of quasifission mass spectra for reactions with nuclei lighter than ^{208}Pb, forming compound systems from Pb to No (Z = 102). For these reactions there should be negligible sequential fission, because the fission barriers of heavy target-like reaction products are high. The

aim was to search for features correlated with the shells known to result in the well-established mass-asymmetric fission commonly seen in low energy fission of actinide nuclides.

Systematic measurements were made at energies near and below the capture barrier (beam energies where quasifission is most prominent [21]) of mass-angle distributions for fission following collisions of ^{48}Ti projectiles with even-even nuclides from ^{154}Sm to ^{200}Hg. Excitation energies above the ground-states ranged from ∼53 to 33 MeV respectively.

To demonstrate the presence of quasifission, selected Mass-Angle Distributions are shown in Fig. 5 (for details see Ref. [49]. The high intensity bands near mass-ratios 0.2 and 0.8 are scattering events with small or no mass exchange. The fission-like events are distributed around mass-ratio 0.5. With increasing compound nucleus atomic number Z_{CN}, a rapid transition occurs from fission having no mass-angle correlation, characteristics of fusion-fission or slow qauasifission (for ^{48}Ti + ^{154}Sm), to predominantly fast quasifission for ^{48}Ti + ^{186} W, and all the heavier targets. This is evidenced by the increasing correlation of the fission M_R distributions with angle: the angled dotted lines highlight the trend of increasing mass-angle correlation for larger Z_{CN}. The four heaviest reactions form ^{234}Cm, ^{240}Cf, ^{244}Fm and ^{248}No, where fission from low excitation energies is expected to be mass-asymmetric, associated with proton shells near Z = 54 [53]. The vertical dot-dashed lines and green arrows indicate this charge-ratio, but no strong correlation of yield here can be seen. In fact peak (angle integrated) quasifission yields are at mass-symmetry for all these reactions, as demonstrated below.

A more detailed analysis was carried out to investigate the possible presence of enhanced quasifission yield at the mass-ratios expected from low energy actinide fission. The location of shell structure in M_R should not change with angle or beam energy. Therefore mass-ratio spectra with the highest statistics available were obtained by integrating over angle from 40° to 140°, and over the lowest three beam energies. These are shown in Fig. 6 for the indicated reactions. In each panel the mean E_x and the mean E/V_B (brackets) are shown.

The lighter C.N. required a two-Gaussian fit, corresponding to fast quasifission (wide) and fusion-fission (narrow). The heavier systems were well-described by a single wide Gaussian (blue curves). Shell effects should result in local deviations from these smooth fits. The location of shells believed to influence fission of nuclei around and lighter than Pb [54–56] is indicated at Z∼36 and 44, as well as Z∼54, known to drive low energy actinide fission.

The heavy nuclei created following capture in these reactions are significantly more neutron-deficient than those generally associated with the Standard I and Standard II modes. To investigate experimentally whether this is important, measured mass spectra converted to M_R (black squares) for low-energy fission of the heaviest elements studied, neutron-deficient ^{242}Cf [50], ^{246}Fm [51] and ^{254}No [52] are shown in Fig. 6(d) to (f). They show similar mass-asymmetric fission to other actinides. The highest yield in each experimental spectrum can be converted to the proton number of the heavy fragment using the UCD assumption, giving an average of Z = 56. Thus if quasifission follows the same shell valley(s) in the PES, the shell structure in quasifission might be expected at M_R values consistent with Z = 56, slightly above the indicated values for Z = 54.

Close inspection of the M_R spectra in Fig. 6 shows that typically one or two points in each spectrum lie consistently above the smooth fits at M_R values slightly higher than the positions of the arrows indicating Z = 54. This deviation corresponds typically to slightly more than one standard deviation, or around 3%. In any one spectrum, this could simply be by chance. However, consistent deviations, not at a fixed M_R but at a variable M_R correlated with expectations for shell effects, would suggest that shells in the heavy fragment might be having a small influence on quasifission mass distributions. However this influence is small, at the limit of sensitivity of the experiment.

In summary, very small (>3%) systematic deviations from smooth behaviour are seen in the quasifission mass spectra at the positions of the known shells. This small influence seems likely to result from attenuation of shell effects due to excitation energy. This is supported by calculations [49] with the semi-empirical GEF model [57], which predict shell effects are negligible at E_X = 30 MeV. These exitation energies are similar to those populated in the ^{50}Ti + actinide reactions discussed earlier, giving reason to expect significant attenuation in those (superheavy element synthesis) reactions also.

5. Conclusions

All the measurements presented for ^{50}Ti + actinide reactions give reason to believe that the observed peak in *binary* quasifission yields around ^{208}Pb results largely from the sequential fission of heavier (actinide) fragments produced in the *primary* quasifission process, resulting in three-body outcomes. In previous measurements of quasifission in SHE synthesis reactions (e.g. Refs. [20,8,58, 23,24,12,1,6]) these events were eliminated by limitations of detector geometrical coverage, and two-body event selection.

Thus the Pb peak seen in binary quasifission mass-spectra cannot presently be taken as giving quantitative evidence for the influence of Pb closed shells on quasifission dynamics. To determine the true effect of the Pb shells on the *primary* quasifission mass spectrum, analysis of all three fragments is clearly desirable, and is currently in progress.

The fall in measured *binary* quasifission yields above the ^{208}Pb peak [20,23,25,1,15,6] for actinide reactions provides separation from deep inelastic reaction products. This separation will be further enhanced by the likelihood of sequential fission following energy dissipation associated with multi-nucleon transfer and (with higher probability) following DIC. The resulting separation seen in *binary* reaction products initially suggested distinct mechanisms for DIC and quasifission. However, measurements published recently where sequential fission is absent because of the lighter target masses [59,5,16] found a continuous distribution of masses and total kinetic energies from deep inelastic products to quasifission. These new results suggest that this is likely true in reactions with actinide nuclides as well.

Another consequence of sequential fission is to make experimental determination of the interaction or capture barrier energies involving fissile actinide nuclides problematic, in the absence of experimental cross-sections for primary quasifission. Using measure-

ments of quasielastic scattering excitation functions [60] eliminates sensitivity to sequential fission of the heavy fragment, but only if the light nucleus is detected in singles. If the heavy nucleus is detected, effects of sequential fission should be considered.

This body of work has shown that understanding and accounting for the effects of sequential fission is very important to allow correct interpretation of superheavy element synthesis reaction measurements. Clarification of mass and energy flows in actinide-based superheavy element synthesis reactions will allow better tests of models, leading to more accurate predictions of optimal reactions for the production of new superheavy elements and isotopes.

CRediT authorship contribution statement

D.J. Hinde: Conceptualization, Formal analysis, Funding acquisition, Investigation, Methodology, Project administration, Resources, Supervision, Validation, Visualization, Writing – original draft, Writing – review & editing. **D.Y. Jeung:** Formal analysis, Investigation, Software, Visualization, Data curation. **M. Dasgupta:** Funding acquisition, Investigation, Resources, Supervision, Writing – review & editing. **J. Buete:** Data curation, Formal analysis, Investigation, Software. **K.J. Cook:** Investigation. **C. Simenel:** Investigation. **E.C. Simpson:** Investigation, Writing – review & editing. **H.M. Albers:** Investigation. **Ch.E. Düllmann:** Investigation, Writing – review & editing. **J. Khuyagbaatar:** Investigation, Writing – review & editing. **A. Yakushev:** Investigation, Resources.

Declaration of competing interest

The authors declare that they have no known competing financial interests or personal relationships that could have appeared to influence the work reported in this paper.

Acknowledgements

The authors acknowledge The Australian Research Council for support through DECRA Fellowship DE230100197 and Discovery grants DP170102318, DP190101442, DP190100256, DP200100601, and DP230101028. Financial support for accelerator operations was provided by the Australian National Collaborative Research Infrastructure Strategy (NCRIS) through the Heavy Ion Accelerators (HIA) project. The authors acknowledge the support of the German academic exchange service (DAAD) via funds of the German Federal Ministry of Education and Research (BMBF).

Data availability

Data will be made available on request.

References

[1] E.M. Kozulin, G.N. Knyazheva, I.M. Itkis, M.G. Itkis, A.A. Bogachev, E.V. Chernysheva, L. Krupa, F. Hanappe, O. Dorvaux, L. Stuttgé, W.H. Trzaska, C. Schmitt, G. Chubarian, Fusion-fission and quasifission of superheavy systems with Z = 110–116 formed in ^{48}Ca-induced reactions, Phys. Rev. C 90 (2014) 054608, https://doi.org/10.1103/physrevc.90.054608.

[2] E.M. Kozulin, G.N. Knyazheva, K.V. Novikov, I.M. Itkis, M.G. Itkis, S.N. Dmitriev, Y.T. Oganessian, A.A. Bogachev, N.I. Kozulina, I. Harca, W.H. Trzaska, T.K. Ghosh, Fission and quasifission of composite systems with Z = 108-120: Transition from heavy-ion reactions involving S and Ca to Ti and Ni ions, Phys. Rev. C 94 (2016) 054613, https://doi.org/10.1103/physrevc.94.054613.

[3] E.M. Kozulin, G.N. Knyazheva, T.K. Ghosh, A. Sen, I.M. Itkis, M.G. Itkis, K.V. Novikov, I.N. Diatlov, I.V. Pchelintsev, C. Bhattacharya, S. Bhattacharya, K. Banerjee, E.O. Saveleva, I.V. Vorobiev, Fission and quasifission of the composite system Z = 114 formed in heavy-ion reactions at energies near the Coulomb barrier, Phys. Rev. C 99 (2019) 014616, https://doi.org/10.1103/physrevc.99.014616.

[4] I.M. Itkis, E.M. Kozulin, M.G. Itkis, G.N. Knyazheva, A.A. Bogachev, E.V. Chernysheva, L. Krupa, Y.T. Oganessian, V.I. Zagrebaev, A.Y. Rusanov, F. Gönnenwein, O. Dorvaux, L. Stuttgé, F. Hanappe, E. Vardaci, E. de Goés Brennand, Fission and quasifission modes in heavy-ion-induced reactions leading to the formation of Hs*, Phys. Rev. C 83 (2011) 064613, https://doi.org/10.1103/PhysRevC.83.064613.

[5] K. Banerjee, D.J. Hinde, M. Dasgupta, E.C. Simpson, D.Y. Jeung, C. Simenel, B.M.A. Swinton-Bland, E. Williams, I.P. Carter, K.J. Cook, H.M. David, Ch.E. Düllmann, J. Khuyagbaatar, B. Kindler, B. Lommel, E. Prasad, C. Sengupta, J.F. Smith, K. Vo-Phuoc, J. Walshe, A. Yakushev, Mechanisms Suppressing Superheavy Element Yields in Cold Fusion Reactions, Phys. Rev. Lett. 122 (2019) 232503, https://doi.org/10.1103/physrevlett.122.232503.

[6] K. Banerjee, D.J. Hinde, M. Dasgupta, J. Sadhukhan, E.C. Simpson, D.Y. Jeung, C. Simenel, B.M.A. Swinton-Bland, E. Williams, L.T. Bezzina, I.P. Carter, K.J. Cook, H.M. Albers, Ch.E. Düllmann, J. Khuyagbaatar, B. Kindler, B. Lommel, C. Mokry, E. Prasad, J. Runke, N. Schunck, C. Sengupta, J.F. Smith, P. Thorle-Pospiech, N. Trautmann, K. Vo-Phuoc, J. Walshe, A. Yakushev, Sensitive search for near-symmetric and super-asymmetric fusion-fission of the superheavy element flerovium (z = 114), Phys. Lett. B 820 (2021) 136601, https://doi.org/10.1016/j.physletb.2021.136601.

[7] V. Zagrebaev, W. Greiner, Cross sections for the production of superheavy nuclei, Nucl. Phys. A 944 (2015) 257–307, https://doi.org/10.1016/j.nuclphysa.2015.02.010.

[8] W.Q. Shen, J. Albinski, A. Gobbi, S. Gralla, K.D. Hildenbrand, N. Herrmann, J. Kuzminski, W.F.J. Müller, H. Stelzer, J. Töke, B.B. Back, S. Bjørnholm, S.P. Sørensen, Fission and quasifission in U-induced reactions, Phys. Rev. C 36 (1987) 115–142, https://doi.org/10.1103/PhysRevC.36.115.

[9] R. du Rietz, D.J. Hinde, M. Dasgupta, R.G. Thomas, L.R. Gasques, M. Evers, N. Lobanov, A. Wakhle, Predominant time scales in fission processes in reactions of s, ti and ni with w: Zeptosecond versus attosecond, Phys. Rev. Lett. 106 (2011) 052701, https://doi.org/10.1103/PhysRevLett.106.052701.

[10] D.J. Hinde, Neutron emission as a clock and thermometer to probe the dynamics of fusion-fission and quasi-fission, Nucl. Phys. A 553 (1993) 255c–270c, https://doi.org/10.1016/0375-9474(93)90627-a.

[11] R. du Rietz, E. Williams, D.J. Hinde, M. Dasgupta, M. Evers, C.J. Lin, D.H. Luong, C. Simenel, A. Wakhle, Mapping quasifission characteristics and timescales in heavy element formation reactions, Phys. Rev. C 88 (2013) 054618, https://doi.org/10.1103/PhysRevC.88.054618.

[12] A. Wakhle, C. Simenel, D.J. Hinde, M. Dasgupta, M. Evers, D.H. Luong, R. du Rietz, E. Williams, Interplay between Quantum Shells and Orientation in Quasifission, Phys. Rev. Lett. 113 (2014) 182502, https://doi.org/10.1103/physrevlett.113.182502.

[13] K. Hammerton, Z. Kohley, D.J. Hinde, M. Dasgupta, A. Wakhle, E. Williams, V.E. Oberacker, A.S. Umar, I.P. Carter, K.J. Cook, J. Greene, D.Y. Jeung, D.H. Luong, S.D. McNeil, C.S. Palshetkar, D.C. Rafferty, C. Simenel, K. Stiefel, Reduced quasifission competition in fusion reactions forming neutron-rich heavy elements, Phys. Rev. C 91 (2015) 041602, https://doi.org/10.1103/physrevc.91.041602.

[14] E. Prasad, D.J. Hinde, E. Williams, M. Dasgupta, I.P. Carter, K.J. Cook, D.Y. Jeung, D.H. Luong, C.S. Palshetkar, D.C. Rafferty, K. Ramachandran, C. Simenel, A. Wakhle, Fusion and quasifission studies for the ^{40}Ca + ^{186}W, ^{192}Os reactions, Phys. Rev. C 96 (2017) 034608, https://doi.org/10.1103/physrevc.96.034608.

[15] H.M. Albers, J. Khuyagbaatar, D.J. Hinde, I.P. Carter, K.J. Cook, M. Dasgupta, Ch.E. Düllmann, K. Eberhardt, D.Y. Jeung, S. Kalkal, B. Kindler, N.R. Lobanov, B. Lommel, C. Mokry, E. Prasad, D.C. Rafferty, J. Runke, K. Sekizawa, C. Sengupta, C. Simenel, E.C. Simpson, J.F. Smith, P. Thörle-Pospiech, N. Trautmann, K. Vo-Phuoc, J. Walshe, E. Williams, A. Yakushev, Zeptosecond contact times for element Z = 120 synthesis, Phys. Lett. B 808 (2020) 135626, https://doi.org/10.1016/j.physletb.2020.135626.

[16] T. Tanaka, D.J. Hinde, M. Dasgupta, E. Williams, K. Vo-Phuoc, C. Simenel, E.C. Simpson, D.Y. Jeung, I.P. Carter, K.J. Cook, N.R. Lobanov, D.H. Luong, C. Palshetkar, D.C. Rafferty, K. Ramachandran, Mass equilibration and fluctuations in the angular momentum dependent dynamics of heavy element synthesis reactions, Phys. Rev. Lett. 127 (2021) 222501, https://doi.org/10.1103/PhysRevLett.127.222501.

[17] T. Tanaka, D.J. Hinde, M. Dasgupta, E. Williams, K. Vo-Phuoc, C. Simenel, E.C. Simpson, D.Y. Jeung, I.P. Carter, K.J. Cook, N.R. Lobanov, D.H. Luong, C. Palshetkar, D.C. Rafferty, K. Ramachandran, Competition between fusion and quasifission in the angular momentum dependent dynamics of heavy element synthesis reactions, Phys. Rev. C 107 (2023) 054601, https://doi.org/10.1103/PhysRevC.107.054601, https://link.aps.org/doi/10.1103/PhysRevC.107.054601.

[18] K.J. Cook, D.C. Rafferty, D.J. Hinde, E.C. Simpson, M. Dasgupta, L. Corradi, M. Evers, E. Fioretto, D. Jeung, N. Lobanov, D.H. Luong, T. Mijatović, G. Montagnoli, A.M. Stefanini, S. Szilner, Colliding heavy nuclei take multiple identities on the path to fusion, Nat. Commun. 14 (1) (2023), https://doi.org/10.1038/s41467-023-43817-8.

[19] B.B. Back, Complete fusion and quasifission in reactions between heavy ions, Phys. Rev. C 31 (1985) 2104, https://doi.org/10.1103/PhysRevC.31.2104.

[20] J. Tōke, B. Bock, G.X. Dai, A. Gobbi, S. Gralla, K.D. Hildenbrand, J. Kuzminski, W.F.J. Müller, A. Olmi, H. Stelzer, Quasi-fission – The mass-drift mode in heavy-ion reactions, Nucl. Phys. A 440 (1985) 327–365, https://doi.org/10.1016/0375-9474(85)90344-6.

[21] D.J. Hinde, M. Dasgupta, E.C. Simpson, Experimental studies of the competition between fusion and quasifission in the formation of heavy and superheavy nuclei, Prog. Part. Nucl. Phys. 118 (2021) 103856, https://doi.org/10.1016/j.ppnp.2021.103856.

[22] P. Gippner, K.D. Schilling, W. Seidel, F. Stary, E. Will, H. Sodan, S.M. Lukyanov, V.S. Salamatin, Y.E. Penionzhkevich, G.G. Chubarian, R. Schmidt, Shell effects in the evolution of the mass asymmetry in heavy-ion collisions leading to composite systems Z = 108, Z. Phys. A 325 (1986) 335–346, https://doi.org/10.1007/bf01294618.

[23] M.G. Itkis, Y.T. Oganessian, V.I. Zagrebaev, Fission barriers of superheavy nuclei, Phys. Rev. C 65 (2002) 044602, https://doi.org/10.1103/physrevc.65.044602.

[24] D.J. Hinde, R. du Rietz, M. Dasgupta, R.G. Thomas, L.R. Gasques, Two Distinct Quasifission Modes in the ^{32}S + ^{232}Th Reaction, Phys. Rev. Lett. 101 (2008) 092701, https://doi.org/10.1103/PhysRevLett.101.092701.

[25] K. Nishio, S. Mitsuoka, I. Nishinaka, H. Makii, Y. Wakabayashi, H. Ikezoe, K. Hirose, T. Ohtsuki, Y. Aritomo, S. Hofmann, Fusion probabilities in the reactions ^{40,48}Ca+ ^{238}U at energies around the Coulomb barrier, Phys. Rev. C 86 (2012) 034608, https://doi.org/10.1103/PhysRevC.86.034608.

[26] G.N. Knyazheva, I.M. Itkis, E.M. Kozulin, The time scale of quasifission process in reactions with heavy ions, J. Phys. Conf. Ser. 515 (2014) 012009, https://doi.org/10.1088/1742-6596/515/1/012009.

[27] M. Morjean, D.J. Hinde, C. Simenel, D.Y. Jeung, M. Airiau, K.J. Cook, M. Dasgupta, A. Drouart, D. Jacquet, S. Kalkal, C.S. Palshetkar, E. Prasad, D. Rafferty, E.C. Simpson, L. Tassan-Got, K. Vo-Phuoc, E. Williams, Evidence for the Role of Proton Shell Closure in Quasifission Reactions from X-Ray Fluorescence of Mass-Identified Fragments, Phys. Rev. Lett. 119 (2017) 222502, https://doi.org/10.1103/physrevlett.119.222502.

[28] Y. Aritomo, Fusion hindrance and roles of shell effects in superheavy mass region, Nucl. Phys. A 780 (3) (2006) 222–246, https://doi.org/10.1016/j.nuclphysa.2006.09.018.

[29] G. Guarino, A. Gobbi, K. Hildenbrand, W. Möller, A. Olmi, H. Sann, S. Bjørnholm, G. Rudolf, Mass drift in reactions between a heavy and a light nucleus, Nucl. Phys. A 424 (1984) 157–183, https://doi.org/10.1016/0375-9474(84)90133-7.

[30] J.V. Kratz, A.E. Norris, G.T. Seaborg, Mass-yield distributions in the reaction of ^{84}Kr ions with ^{238}U, Phys. Rev. Lett. 33 (1974) 502–505, https://doi.org/10.1103/PhysRevLett.33.502.

[31] J.V. Kratz, J.O. Liljenzin, A.E. Norris, G.T. Seaborg, Charge and mass distributions in the reaction of ^{40}Ar ions with ^{238}U, Phys. Rev. C 13 (1976) 2347–2365, https://doi.org/10.1103/physrevc.13.2347.

[32] P. Vater, E. Khan, R. Beckmann, P. Gottschalk, R. Brandt, Sequential fission studies in the interaction of 9.03 MeV/n 238u with natU using mica track detectors, Int. J. Radiat. Appl. Instrum., Part D, Nucl. Tracks Radiat. Meas. 11 (1–2) (1986) 5–16, https://doi.org/10.1016/1359-0189(86)90014-2.

[33] R.J. Charity, R. Freifelder, A. Gobbi, N. Hermann, K.D. Hildenbrand, F. Rami, H. Stelzer, J.P. Wessels, G. Casini, P.R. Maurenzig, A. Olmi, A.A. Stefanini, J. Galin, D. Guerreau, U. Jahnke, A. Peghaire, J.C. Adloff, B. Bilwes, R. Bilwes, G. Rudolf, M. Petrovici, M. Gnirs, D. Pelte, Results on 2-body, 3-body, and 4-body events from the mo-100+mo-100 and sn-120+sn-120 collisions around e/a = 20 mev, Z. Phys. A Hadrons Nucl. 341 (1) (1991) 53–73, https://doi.org/10.1007/BF01281274.

[34] A.A. Stefanini, G. Casini, P.R. Maurenzig, A. Olmi, R.J. Charity, R. Freifelder, A. Gobbi, N. Herrmann, K.D. Hildenbrand, M. Petrovici, F. Rami, H. Stelzer, J.P. Wessels, M. Gnirs, D. Pelte, J. Galin, D. Guerreau, U. Jahnke, A. Peghaire, J.C. Adloff, B. Bilwes, R. Bilwes, G. Rudolf, Analysis of the sequential fission observed in collisions of 100mo + 100mo and 120sn + 120sn around 20 a MeV, Z. Phys. A Hadrons Nucl. 351 (2) (1995) 167–186, https://doi.org/10.1007/bf01289527.

[35] K.V. Novikov, E.M. Kozulin, G.N. Knyazheva, I.M. Itkis, M.G. Itkis, A.A. Bogachev, I.N. Diatlov, M. Cheralu, D. Kumar, N.I. Kozulina, A.N. Pan, I.V. Pchelintsev, I.V. Vorobiev, W.H. Trzaska, S. Heinz, H.M. Devaraja, B. Lommel, E. Vardaci, S. Spinosa, A. Di Nitto, A. Pulcini, S.V. Khlebnikov, P.P. Singh, R.N. Sahoo, B. Gall, Z. Asfari, C. Borcea, I. Harca, D.M. Filipescu, Investigation of fusion probabilities in the reactions with ^{52,54}Cr,^{64} Ni, and ^{68}Zn ions leading to the formation of $z = 120$ superheavy composite systems, Phys. Rev. C 102 (2020) 044605, https://doi.org/10.1103/PhysRevC.102.044605.

[36] D.Y. Jeung, D.J. Hinde, E. Williams, M. Dasgupta, E.C. Simpson, R. du Rietz, D.H. Luong, R. Rafiei, M. Evers, I.P. Carter, K. Ramachandran, C. Palshetkar, D.C. Rafferty, C. Simenel, A. Wakhle, Energy dissipation and suppression of capture cross sections in heavy ion reactions, Phys. Rev. C 103 (2021) 034603, https://doi.org/10.1103/PhysRevC.103.034603.

[37] D.Y. Jeung, D.J. Hinde, M. Dasgupta, C. Simenel, E.C. Simpson, K.J. Cook, H.M. Albers, J. Buete, I.P. Carter, C.E. Düllmann, J. Khuyagbaatar, B. Kindler, N. Lobanov, B. Lommel, C. Mokry, E. Prasad, J. Runke, C. Sengupta, J.F. Smith, P. Thörle-Pospiech, N. Trautmann, K. Vo-Phuoc, J. Walshe, E. Williams, A. Yakushev, Sequential fission and the influence of 208pb closed shells on the dynamics of superheavy element synthesis reactions, Phys. Lett. B 837 (2023) 137641, https://doi.org/10.1016/j.physletb.2022.137641.

[38] N.R. Lobanov, P. Linardakis, D. Tempra, Bunching and chopping for tandem accelerators. part i: Bunching, Nucl. Instrum. Methods Phys. Res. Sect. B Beams Interact. Mater. Atoms 499 (2021) 133–141, https://doi.org/10.1016/j.nimb.2021.02.013.

[39] N.R. Lobanov, P. Linardakis, D. Tempra, Bunching and chopping for tandem accelerators. part ii:Chopping, Nucl. Instrum. Methods Phys. Res. Sect. B Beams Interact. Mater. Atoms 499 (2021) 142–147, https://doi.org/10.1016/j.nimb.2021.02.014.

[40] W.J. Świątecki, K. Siwek-Wilczyńska, J. Wilczyński, Fusion by diffusion. II. Synthesis of transfermium elements in cold fusion reactions, Phys. Rev. C 71 (2005) 014602, https://doi.org/10.1103/physrevc.71.014602.

[41] D.J. Hinde, M. Dasgupta, J.R. Leigh, J.C. Mein, C.R. Morton, J.O. Newton, H. Timmers, Conclusive evidence for the influence of nuclear orientation on quasifission, Phys. Rev. C 53 (1996) 1290–1300, https://doi.org/10.1103/PhysRevC.53.1290.

[42] R.G. Thomas, D.J. Hinde, D. Duniec, F. Zenke, M. Dasgupta, M.L. Brown, M. Evers, L.R. Gasques, M.D. Rodriguez, A. Diaz-Torres, Entrance channel dependence of quasifission in reactions forming ^{220}Th, Phys. Rev. C 77 (2008) 034610, https://doi.org/10.1103/PhysRevC.77.034610.

[43] T. Banerjee, D.J. Hinde, D.Y. Jeung, K. Banerjee, M. Dasgupta, A.C. Berriman, L.T. Bezzina, H.M. Albers, Ch.E. Düllmann, J. Khuyagbaatar, B. Kindler, B. Lommel, E.C. Simpson, C. Sengupta, B.M.A. Swinton-Bland, T. Tanaka, A. Yakushev, K. Eberhardt, C. Mokry, J. Runke, P. Thörle-Pospiech, N. Trautmann, Systematic evidence for quasifission in ^{9}Be -, ^{12}C -, and ^{16}O - induced reactions forming ^{258,260}No, Phys. Rev. C 102 (2020) 024603, https://doi.org/10.1103/physrevc.102.024603.

[44] D.J. Hinde, R. du Rietz, M. Dasgupta, R.G. Thomas, L.R. Gasques, Two Distinct Quasifission Modes in the ^{32}S + ^{232}Th Reaction, Phys. Rev. Lett. 101 (2008) 092701, https://doi.org/10.1103/PhysRevLett.101.092701.

[45] R. du Rietz, D.J. Hinde, M. Dasgupta, R.G. Thomas, L.R. Gasques, M. Evers, N. Lobanov, A. Wakhle, Predominant Time Scales in Fission Processes in Reactions of S, Ti and Ni with W: Zeptosecond versus Attosecond, Phys. Rev. Lett. 106 (2011) 052701, https://doi.org/10.1103/PhysRevLett.106.052701.

[46] E. Prasad, A. Wakhle, D.J. Hinde, E. Williams, M. Dasgupta, M. Evers, D.H. Luong, G. Mohanto, C. Simenel, K. Vo-Phuoc, Exploring quasifission characteristics for ^{34}S + ^{232}Th forming ^{266}Sg, Phys. Rev. C 93 (2016) 024607, https://doi.org/10.1103/PhysRevC.93.024607.

[47] D.J. Hinde, J.R. Leigh, J.J.M. Bokhorst, J.O. Newton, R.L. Walsh, J.W. Boldeman, Mass-split dependence of the pre- and post-scission neutron multiplicities for fission of 251es, Nucl. Phys. A 472 (2) (1987) 318–332, https://doi.org/10.1016/0375-9474(87)90213-2.

[48] D.J. Hinde, D.Y. Jeung, E. Prasad, A. Wakhle, M. Dasgupta, M. Evers, D.H. Luong, R. du Rietz, C. Simenel, E.C. Simpson, E. Williams, Sub-barrier quasifission in heavy element formation reactions with deformed actinide target nuclei, Phys. Rev. C 97 (2018) 024616, https://doi.org/10.1103/physrevc.97.024616.

[49] D.J. Hinde, R. du Rietz, D.Y. Jeung, K.J. Cook, M. Dasgupta, E.C. Simpson, R.G. Thomas, M. Evers, C.J. Lin, D.H. Luong, L.R. Gasques, R. Rafiei, A. Wakhle, C. Simenel, Experimental investigation of the role of shell structure in quasifission mass distributions, Phys. Rev. C 106 (2022) 064614, https://doi.org/10.1103/PhysRevC.106.064614, https://link.aps.org/doi/10.1103/PhysRevC.106.064614.

[50] D.A. Shaughnessy, J.L. Adams, K.E. Gregorich, M.R. Lane, C.A. Laue, D.M. Lee, C.A. McGrath, J.B. Patin, D.A. Strellis, E.R. Sylwester, P.A. Wilk, D.C. Hoffman, Electron-capture delayed fission properties of ^{242}Es, Phys. Rev. C 61 (4) (mar 2000), https://doi.org/10.1103/physrevc.61.044609.

[51] D. Hoffman, D. Lee, A. Ghiorso, M. Nurmia, K. Aleklett, Fragment mass and kinetic-energy distributions from spontaneous fission of the neutron-deficient isotopes, 1.2-s ^{246}Fm and 38-s ^{248}Fm, Phys. Rev. C 22 (1980) 1581–1584, https://doi.org/10.1103/PhysRevC.22.1581, https://link.aps.org/doi/10.1103/PhysRevC.22.1581.

[52] J. Wild, E. Hulet, R. Lougheed, K. Moody, B. Bandong, R. Dougan, A. Veeck, Spontaneous fission properties of 252,254no and 256,258[104] and the disappearance of the outer fission barrier, J. Alloys Compd. 213–214 (1994) 86–92, https://doi.org/10.1016/0925-8388(94)90885-0.

[53] C. Bockstiegel, S. Steinhauser, K.-H. Schmidt, H.-G. Clerc, A. Grewe, A. Heinz, M. de Jong, A. Junghans, J. Muller, B. Voss, Nuclear-fission studies with relativistic secondary beams: Analysis of fission channels, Nucl. Phys. A 802 (1–4) (2008) 12–25, https://doi.org/10.1016/j.nuclphysa.2008.01.012.

[54] E. Prasad, D.J. Hinde, M. Dasgupta, D.Y. Jeung, A.C. Berriman, B.M.A. Swinton-Bland, C. Simenel, E.C. Simpson, R. Bernard, E. Williams, K.J. Cook, D.C. Rafferty, C. Sengupta, J.F. Smith, K. Vo-Phuoc, J. Walshe, Systematics of the mass-asymmetric fission of excited nuclei from ^{176}Os to ^{206}Pb, Phys. Lett. B 811 (2020) 135941, https://doi.org/10.1016/j.physletb.2020.135941.

[55] B.M.A. Swinton-Bland, J. Buete, D.J. Hinde, M. Dasgupta, T. Tanaka, A.C. Berriman, D.Y. Jeung, K. Banerjee, L.T. Bezzina, I.P. Carter, K.J. Cook, C. Sengupta, C. Simenel, E.C. Simpson, M.A. Stoyer, Multi-modal mass-asymmetric fission of 178pt from simultaneous mass-kinetic energy fitting, Phys. Lett. B 837 (2023) 137655, https://doi.org/10.1016/j.physletb.2022.137655.

[56] K. Mahata, C. Schmitt, S. Gupta, A. Shrivastava, G. Scamps, K.-H. Schmidt, Evidence for the general dominance of proton shells in low-energy fission, Phys. Lett. B 825 (2022) 136859, https://doi.org/10.1016/j.physletb.2021.136859.

[57] K.-H. Schmidt, B. Jurado, C. Amouroux, C. Schmitt, General description of fission observables: Gef model code, Nucl. Data Sheets 131 (2016) 107–221, https://doi.org/10.1016/j.nds.2015.12.009, special Issue on Nuclear Reaction Data.

[58] M.G. Itkis, Y.T. Oganessian, E.M. Kozulin, A.A. Bogatchev, I. Itkis, M. Jamdel, J. Kliman, G. Kniajeva, N.A. Kondratiev, J.V. Korzyukov, L. Krupa, I.V. Povrovski, V.A. Ponomarenko, E.V. Prokhorova, A.Y. Rusanov, V.M. Voskresenski, F. Hanappe, B. Benoit, T. Materna, N. Rowley, L. Stuttge, G. Giardina, K.J. Moody, Shell effects and the fission of superheavy nuclei at low excitation energies, in: Preprint E15-99-248, Dubna, Joint Inst. of Nuclear Research, 1999, pp. 1–10.

[59] E. Williams, K. Sekizawa, D.J. Hinde, C. Simenel, M. Dasgupta, I.P. Carter, K.J. Cook, D.Y. Jeung, S.D. McNeil, C.S. Palshetkar, D.C. Rafferty, K. Ramachandran, A. Wakhle, Exploring Zeptosecond Quantum Equilibration Dynamics: From Deep-Inelastic to Fusion-Fission Outcomes in ^{58}Ni + ^{60}Ni Reactions, Phys. Rev. Lett. 120 (2018) 022501, https://doi.org/10.1103/physrevlett.120.022501.

[60] T. Tanaka, K. Morita, K. Morimoto, D. Kaji, H. Haba, R. Boll, N. Brewer, S.V. Cleve, D. Dean, S. Ishizawa, Y. Ito, Y. Komori, K. Nishio, T. Niwase, B. Rasco, J. Roberto, K. Rykaczewski, H. Sakai, D. Stracener, K. Hagino, Study of Quasielastic Barrier Distributions as a Step towards the Synthesis of Superheavy Elements with Hot Fusion Reactions, Phys. Rev. Lett. 124 (2020) 052502, https://doi.org/10.1103/PhysRevLett.124.052502.